Non-resonant destabilization of (1/1) internal kink mode by suprathermal electron pressure

Citation: Delgado-Aparicio, L. et al. "Non-Resonant Destabilization of (1/1) Internal Kink Mode by Suprathermal Electron Pressure." Physics of Plasmas 22, 5 (May 2015): 050701 © 2015 AIP Publishing LLC

As Published: http://dx.doi.org/10.1063/1.4919964

Publisher: American Institute of Physics (AIP)

Persistent URL: http://hdl.handle.net/1721.1/113079

Version: Author's final manuscript: final author's manuscript post peer review, without publisher's formatting or copy editing

Non-Resonant Destabilization Of $(1/1)$ Internal Kink Mode By Suprathermal Electron Pressure

L. Delgado-Aparicio[1], L. Sugiyama[2], S. Shiraiwa[3], J. Irby[3], R. Granetz[3], R. Parker[3], S. G. Baek[3], I. Faust[3], G. Wallace[3], D. A. Gates[1], N. Gorelenkov[1], R. Mumgaard[3], S. Scott[1], N. Bertelli[1], C. Gao[3], M. Greenwald[3], A. Hubbard[3], J. Hughes[3], E. Marmar[3], P. E. Phillips[4], J. E. Rice[3], W. L. Rowan[4], R. Wilson[1], S. Wolfe[3] and S. Wukitch[31]

[1] *Princeton Plasma Physics Laboratory, Princeton, NJ, 08540, USA*
[2] *MIT - Laboratory of Nuclear Science, Cambridge, MA, 02139, USA*
[3] *MIT - Plasma Science and Fusion Center, Cambridge, MA, 02139, USA*
[4] *University of Texas at Austin, Austin, TX, 78712, USA*

(Dated: 28 April 2015)

New experimental observations are reported on the structure and dynamics of short-lived periodic $(1,1)$ "fishbone"-like oscillations that appear during radio frequency heating and current-drive experiments in tokamak plasmas. For the first time, measurements can directly relate changes in the high energy electrons to the mode onset, saturation, and damping. In the relatively high collisionality of Alcator C-Mod with lower hybrid current drive, the instability appears to be destabilized by the non-resonant suprathermal electron pressure - rather than by wave-particle resonance, rotates toroidally with the plasma and grows independently of the $(1,1)$ sawtooth crash driven by the thermal plasma pressure.

PACS numbers: 52.55.Fa, 52.35.Py, 52.50.Sw, 52.55.Tn 52.55.Wq

The economic feasibility of a fusion reactor can be measured in terms of $\beta \equiv p/\left(B^2/2\mu_0\right)$, where p is the plasma pressure and $B^2/2\mu_0$ is the magnetic field energy density. The presence of magnetohydrodynamic (MHD) instabilities can distort the orbits of fast ions and electrons compared to the equilibrium, causing an off-axis redistribution of the fusion heating and current density to the detriment of the central β, reducing the fusion power and the production of fast neutrons for tritium breeding. Therefore, understanding the stability and behavior of 3D helical modes in the core of an axisymmetric toroidal configuration remains one of the challenges of fusion research[1–6]. It is doubly significant for burning plasmas such as ITER, where the $q = 1$ radius that bounds these instabilities may reach half the minor radius.

A helical internal kink-like mode[7–9] with dominant poloidal and toroidal mode numbers $m = 1$, $n = 1$ has recently been observed in the Alcator C-Mod tokamak[10], during the development of advanced fusion scenarios using lower hybrid current drive (LHCD)[11–13]. During LHCD operation, soft x-ray (SXR) detectors measure periodic bursts of oscillations as shown in Fig. 1. These have a (1,1) structure characterized by a small helical, internal-kink-like region of enhanced plasma density and temperature that is radially concentrated on or inside the $q = 1$ surface and rotates toroidally with the plasma.

The (1,1) internal-kink (IK) bursts are distinct from the sawtooth instability. In Figure 1-a) the instability occurs once during the sawtooth ramp and disappears before the subsequent sawtooth crash. In Figure 1-b) sawteeth are absent and the fishbone-like mode appears as a successive train of bursts. The growth and amplitude are nearly identical in both cases; however, the amplitude of the off-axis re-distribution is different from that of the sawtooth crash (SC). Growth and damping of the mode

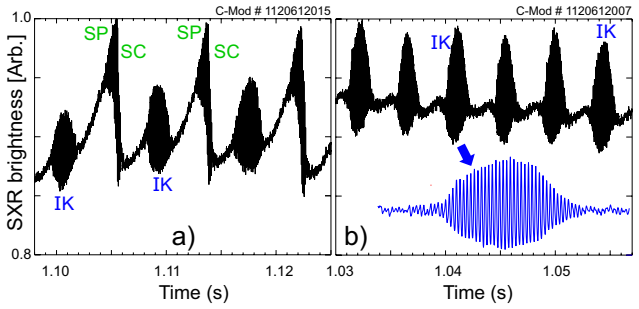

FIG. 1. (Color online) On-axis SXR signatures of a (1,1) internal kink-like (IK) mode in the a) presence or b) absence of sawtooth precursors (SP) and crashes (SC). The inset shown in -b) is an expanded time trace of an IK burst where the slow DC offset has been removed for clarity.

occur over approximately 1 ms intervals, similar to the growth time of the sawtooth precursor and much longer than the 20-40 μs of the sawtooth crash. On occasions, the mode can coalesce with the precursor oscillations in a "hybrid" crash with larger amplitude as depicted in the spectrogram shown in Fig. 2-a). The integrated power spectrum shows symmetrical, smooth gaussian-shaped growth and damping of the mode compared to the sharper sawtooth crash, and the wider double pulse representing the hybrid crash [see Fig. 2-b)]; in this case, the sawtooth precursor appears to grow from the oscillations remaining from an incompletely damped mode. The three modes have distinct amplitudes, but nearly identical frequencies; small differences may arise from sawtooth recovery as observed in the interaction between sawteeth and long-lived (1,1) modes[4,5]. They propagate toroidally in the counter-current or the electron diamag-

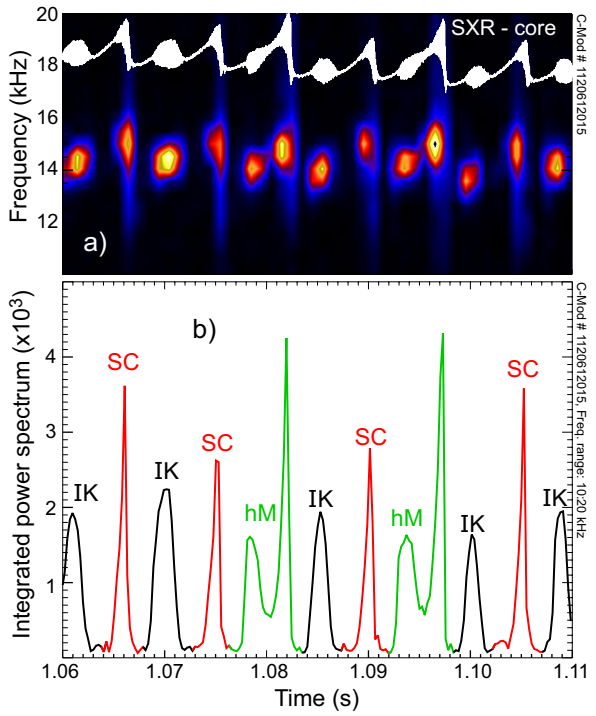

FIG. 2. (Color online) a) Frequency spectrogram of SXR signal from the core (for reference, raw SXR signal is shown in white). b) Integrated power spectrum between 10-20 kHz. The internal kink-like bursts (IK, in black) and sawtooth crashes (SC, in red) can also coexist in a (1,1) hybrid mode (hM, in green).

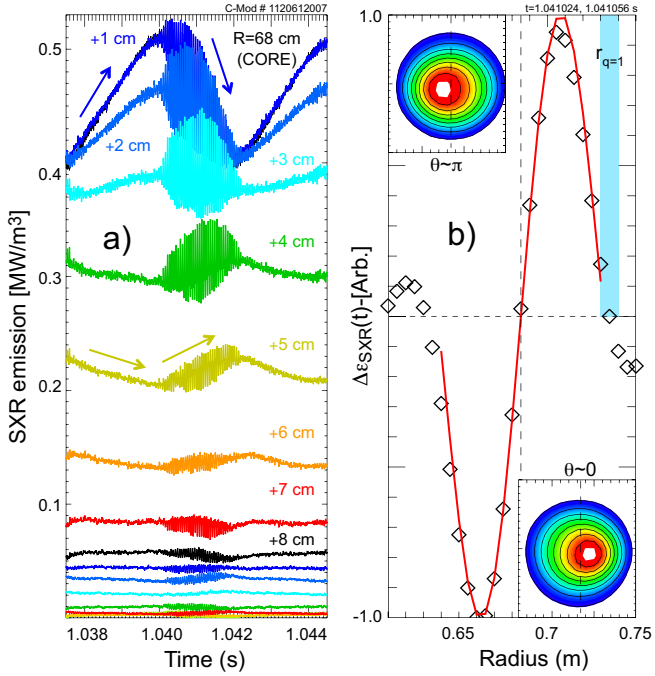

FIG. 3. (Color online) a) Time history of the SXR emissivity over the midplane on the low-field-side. b) SXR perturbation (black diamonds) has the analytical form of the lowest order 1/1 internal kink eigenfunction, Bessel function $J_1(\kappa r)\cos\theta$ with $\kappa = 3.8317/r_{q=1}$ (red line). Reconstructions with the mode at $\theta = 0$ and $\theta = \pi$ are shown in the insets.

netic drift direction, with the same direction and speed as the core plasma rotation, as does the sawtooth precursor. The background toroidal rotation, measured with a high-resolution core x-ray imaging spectrometer (CXIS)[14,15] was 60–75 km/s for the modes shown in Fig. 1.

These observations are from C-Mod plasmas which had $R_0 \simeq 68.5$ cm, $a = 22$ cm, $I_p \simeq 0.5$ MA, $B_{t,0} \simeq 5.4$ T, and central plasma densities and temperatures on the order of $n_{e0} \sim (1.35 \rightarrow 1.75) \times 10^{20}$ m^{-3} and $T_{e,0} \sim 2.80 \rightarrow 2.35$ keV, with nearly identical central electron and ion pressures. Lower hybrid (LH) waves are quasi-electrostatic plasma waves with a frequency intermediate between the electron and ion cyclotron frequencies which are absorbed by relatively fast background electrons via electron Landau damping. The C-Mod LHCD system is capable of driving up to 580 kA of current at zero loop voltage in moderate plasma densities ($\overline{n}_e \sim 5 \times 10^{19}$ m^{-3}). However, at the high densities of these discharges, 700 kW of LH power with a parallel refractive index $n_{||,LHCD} \simeq -1.6$ drove a smaller reduction in the loop voltage, $\Delta V_{loop} \simeq -0.3$ V below the typical C-Mod ohmic $V_{loop} \sim 1$ V. The current density on axis typically reached 14 MA/m^2 with $q_0 \simeq 0.9$; the broad LHCD current and power deposition profiles extended well outside $q = 1$.

The 3D mode structure and its effects on the background plasma were measured using a suite of spectroscopic imaging diagnostics[5]. These instruments were also used to infer the mode harmonic numbers, since the magnetic measurements at the wall were insensitive to interior modes[5]. The spatial time history of the tomographically reconstructed SXR emissivity for a typical kink-like burst from Fig. 1-b) is shown in Fig. 3-a). At the magnetic axis, the background emissivity in the plasma center builds nearly to a peak before the mode onset (see top black and blue traces at $\Delta R = +1$ and 2 cm from the plasma core). In contrast, at $\Delta R = 4$–5 cm the background emissivity falls steadily before the mode onset, then during the mode rises by 10% while the core background emissivity decreases by 20%. There is no signal inversion with radius that might correspond to a "crash" of the central core. 2D reconstructions of the SXR emissivity profiles depicted in Fig. 3-b) shows that the mode forms and then grows like a small amplitude $(1,1)$ kink with a nearly circular cross section. Its radial profile has the characteristic Bessel function form of the cylindrical or lowest order toroidal 1/1 kink eigenfunction[16]. A complete description of the SXR tomographic capability has been published elsewhere (see[5] and references therein). Combining this functional form with data from the ten-chord two-color interferometer (TCI[17]) we infer an internal kink-like electron density perturbation as large as $\delta n_{e0}/n_{e0} \simeq 4\%$ (see Fig. 4). The TCI data also sug-

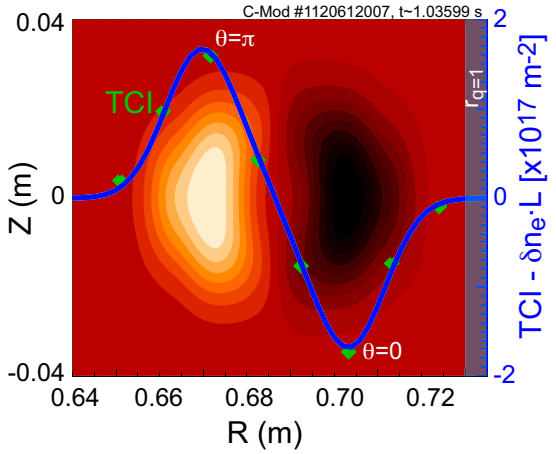

FIG. 4. (Color online) Line-integrated measured (in green) and simulated (in blue) $\tilde{n}_e$ during the sawtooth-free scenario shown in Fig. 1-b). The background shading is the corresponding 2D Bessel-like eigenfunction.

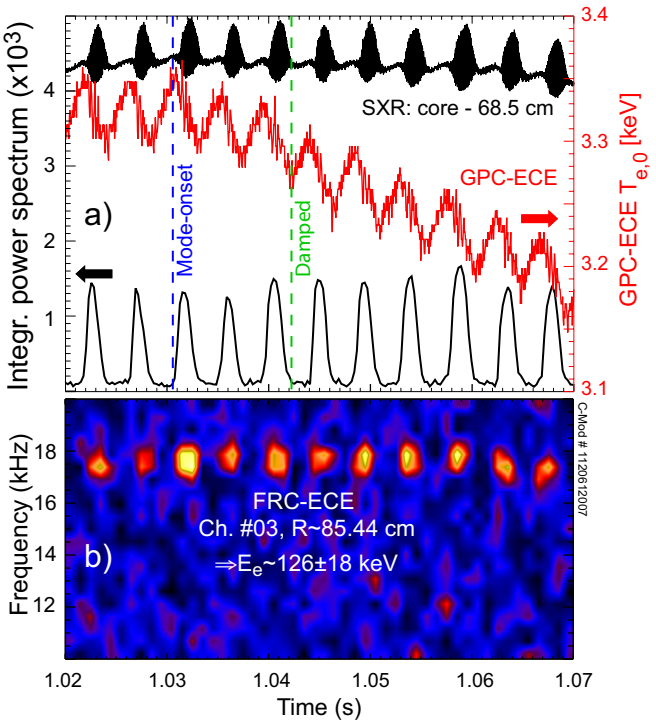

FIG. 5. (Color online) a) Overlay of integrated power spectrum of the SXR signals (for reference raw signal is also shown in black) and $T_{e,0}$ values from the GPC-ECE grating polychromenter (middle curve, red) for the fishbone-like mode. b) Spectrogram of an edge channel of high resolution FRC-ECE radiometer shows MHD activity that is core-localized.

gests that the mode grows smoothly, saturates, and decays, without any reconnection event. The position of the $q = 1$ surface indicated in Figs. 3 and 4 was obtained from an MSE-constrained EFIT reconstruction.

For the first time, experimental measurements demonstrate a direct dynamic relation between LHCD generated fast electrons and a fishbone-like mode. A time history of the central electron temperature inferred by the slow electron cyclotron emission (ECE) grating polychromator (GPC)[18] shows that the mode growth begins at the maximum of the inferred core T_e, which falls to a minimum by the disappearance of the mode [see dotted lines in Fig. 5-a)]. During this sawtooth stabilized scenario the amplitude of the kink-like mode is practically constant with a frequency near that of the plasma toroidal rotation. The high resolution, fast-time-response FRC-ECE radiometer[19] provides additional evidence that fast electrons are connected to the mode onset and evolution, as deduced from Fig. 5-b). Radiation at the second harmonic of the electron cyclotron frequency produced by fast electrons in the central region was detected in a radial channel on the low-field edge nearly 20 cm away from the magnetic axis and only while the mode is active. This apparent mismatch is due to the strong downshift of electron cyclotron frequency by relativistic effects, $\Omega_{ce,rel} = eB/\gamma m_e$ where $\gamma_e \equiv (1 - (v_e/c)^2)^{-1/2}$ is the Lorentz factor[13,20–23]. Electron cyclotron waves emitted in the core at these frequencies can travel to the outboard plasma edge without being re-absorbed by the thermal electrons. Assuming a $1/R$ dependence for the toroidal magnetic field, the relativistic factor is found to be γ_e=1.21-1.28, corresponding to electron energies E_e = 108-144 keV. The calculated energies, mainly from circulating electrons, fall within the range of peak energies expected for LHCD.

The mode appears to be a fishbone-like, (1,1) internal-kink disturbance that smoothly grows, saturates, and decays, without any sign of a "crash" or reconnection event. The instability oscillates predominantly near the frequency of bulk plasma rotation and without chirping. Observed only during LHCD, it appears to be driven by a build-up of LH-generated fast electrons over $q < 1$ and to saturate as they are lost. We argue that this behavior is consistent with an internal kink destabilized by the suprathermal fast-electron pressure (β_e^{hot}). An estimate for the central fast electron pressure, based on the change in the loop-voltage, the central current density, an approximate density of fast electrons, and an average electron energy for parallel velocities between $3v_{th,e}$ and $v_{\parallel,max} = c/n_\parallel$, yields $p_{e0}^{hot} \approx 1.52 \times 10^{19}$ keV·m^{-3}, or 4% of the thermal electron pressure p_{e0}^{th}. A slightly more accurate approach uses the GENRAY/CQL3D suite[11–13,24,25] to calculate the anisotropic electron distribution function $f(v_\parallel, v_\perp)$. The electron pressure is the moment of the velocity distribution, $p_e = \int_0^\infty Ef(E)d^3v$. Writing it as $p_e = \int_0^\infty I(E)dE$, the integrands $I(E)$ can be calculated for ohmic and LHCD heated plasmas as shown in Figs. 6-a) and -b). The difference between the LH and ohmic distributions, plotted in Fig. 6-c) at two radii $r \simeq 0$ and $r_{q=1}$, shows that the LH fast electron pressure comes mainly from en-

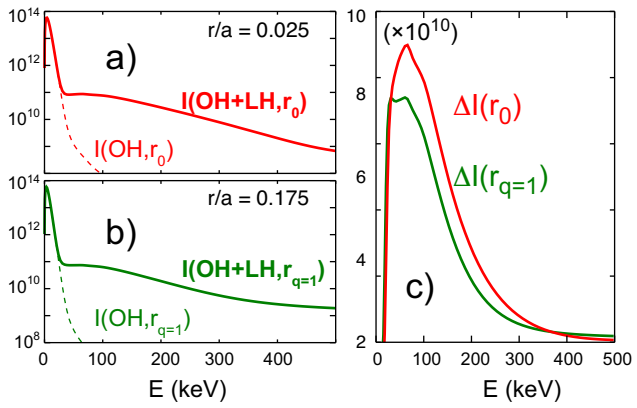

FIG. 6. (Color online) a), b) The integrands I(E) of the central electron pressure for ohmic and LHCD plasmas at two radii r_0 and $r_{q=1}$ and c) their difference, showing the LH fast electron contribution.

ergies between 30 and 200 keV, with a peak around 80 keV. The ratio of the fast electron pressure to the thermal pressure is $p_{e0}^{hot}/p_{e0}^{th} \simeq 2.5\%$ at the magnetic axis, when numerically integrated from $3v_{th,e}$ to 2.5 MeV, and 2.8% at the $q = 1$ surface. This is comparable to the drop in the thermal electron pressure due to the mode, $\Delta p_{e0}^{th}/p_{e0}^{th} \gtrsim 2.75\%$, derived from before and after measurements of the central radiated power density and ECE T_e. Increases in the central β between 2.5 and 4% are theoretically sufficient to destabilize a marginally stable internal kink mode, but are smaller than the typical change over a sawtooth in agreement with the observations.

The C-Mod modes resemble some "electron fishbone" and hybrid "sawbone" (1,1) modes observed with electron cyclotron resonance heating (ECRH) and LHCD in DIII-D[26], FTU[27], Tore Supra[28–30], HT-7[31,32], HL-1M[33], HL-2A[34] and recently EAST[35] and TCV[36]. A number of wave-particle resonant interactions[33,37–42] have been proposed theoretically to explain the mode destabilization in experiments with low-density plasmas ($\overline{n}_e \sim 0.5 - 0.8 \times 10^{19}$ m^{-3}). In some cases, the wave-particle resonance is clear, as for ECRH or ECCD applied on the high field side[26]. In others, parallel or perpendicular resonance was assumed within the framework of existing resonant electron fishbone theory, but its identification remained inconclusive due to the lack of sufficiently precise local measurements. In many cases, the Doppler shift correction to the mode frequency was neglected due to the lack of core toroidal rotation profiles. An appropriate Doppler shift correction of the mode frequency is done in Alcator C-Mod using the plasma toroidal rotation inferred from an x-ray imaging crystal spectrometer[14,15]. Most cases also lacked good measurements of fast-electron dynamics. Estimates of the assumed resonant electron energy and the precession drift frequency are often inferred from changes of the hard x-ray spectrum; however, measured profiles of x-ray emission for specific photon energies are not representative of the actual anisotropic emission distribution, or of the electron distribution function of commensurate energy[23].

Resonant electron fishbone theories postulate a resonance with the toroidal precession drift of the fast trapped and/or barely circulating electrons[39,40]. This can be ruled out for C-Mod LH fishbones at relatively high collisionality; in fact, Alcator C-Mod operates at ITER-like core densities of $1.4 - 1.6 \times 10^{20}$ m^{-3} in which a non-resonant destabilization can be expected. The LH-driven parallel velocity is distributed into the perpendicular direction by collisions, but the rapid de-trapping rate means that very few trapped electrons exist[11]. Thus only circulating electrons contribute to resonance. In C-Mod, however, the barely circulating electrons are a small fraction of the total number of fast electrons, 10-15% based on the GENRAY/CQL3D distribution[9]. This still overestimates the possible resonant contribution since rapid detrapping also implies significant collisional disruption of the circulating orbits and their precession drift. Thus the total resonant drive is a small fraction of the fast electron beta and is unlikely to be able to destabilize the mode. The situation is quite different for the less collisonal cases of high power LH at lower density, as in FTU, or the typically very low density ECH or ECCD fishbones for which the resonant parallel electron theories were proposed. Direct parallel resonances similar to ion parallel fishbones[43] are also unlikely. The LH parallel electron velocities are distributed over a wide range in velocity space, 3-10$v_{th,e}$ ($12 < E < 500$ keV), so that there are relatively few particles at any given resonant velocity. In contrast, ion parallel fishbones[43] in parallel-NBI heated plasmas have a concentrated high power source of fast parallel ions at the beam energy.

Two main possibilities then exist for mode saturation. The non-axisymmetric kink may actively expel fast electrons from $q < 1$ faster than their creation. Unlike ion and most ECRH electron fishbones with large gyro- or trapped-particle orbits, there is no obvious mechanism for strong perpendicular expulsion of fast particles without a core "crash", which is not observed. Electron gyroradii are very small ($\sim$ 1 mm) and almost no trapped particles exist, so fast electrons remain strongly tied to the magnetic field lines. Alternatively, the kink non-axisymmetry could alter the LH wave propagation to exclude power and current drive deposition from the kink region. This scenario is consistent with experimental observations of reduced LHCD efficiency when 3D helical modes appear in the core of tokamak plasmas. The loss time for LH fast electrons near the plasma center due to radial diffusion and other processes is 1–2 ms, similar to the mode growth and decay times. Since the total absorbed LH power remains fairly constant, extra power should be deposited outside $q < 1$, which is consistent with the observed changes in the background SXR and temperature[9]. However, kink effects on the LH power deposition have not been studied theoretically, since numerical calculations in realistic configurations have so far

assumed toroidal axisymmetry.

In summary, a fishbone-like instability with a (1, 1) internal kink-like structure rotating at the background plasma toroidal rotation frequency is observed in high-density scenarios on Alcator C-Mod with LHCD. For the first time, measurements at high spatial and temporal resolution directly connect changes in the fast LH-generated electrons to the mode. Suprathermal electron energies are measured directly using the downshift of electron gyrofrequency due to relativistic effects, and correlate with the mode. The results suggest that the fishbone-like mode is a marginally stable internal kink that is destabilized by the non-resonant suprathermal electron pressure contribution to the central β thus offering an alternative explanation for the mode-onset and evolution for cases where the wave-particle resonances of traditional electron fishbones are weak. The independence of the fast-electron pressure from the thermal pressure that drives the conventional internal kink also explains its varied co-existence with the sawtooth crash and precursor oscillations. This work was performed under US DoE contracts including DE-FC02-99ER54512 and DE-SC0007883 at MIT and DE-AC02-09CH11466 at PPPL

[1] J. Menard, R. E. Bell, D. A. Gates, S. M. Kaye, B. P. LeBlanc, F. M. Levinton, S. S. Medley, S. A. Sabbagh, D. Stutman, K. Tritz, and H. Yuh, Phys. Rev. Letters, **97**, 095002, (2006).

[2] I. T. Chapman, M.-D. Hua, S. D. Pinches, R. J. Akers, A. R. Field, J. P. Graves, R. J. Hastie, C. A. Michael and the MAST Team, Nucl. Fusion, **50**, 045007, (2010).

[3] D. P. Brennan, C. C. Kim and R. J. La Haye, Nucl. Fusion, **52**, 033004, (2012).

[4] L. Delgado-Aparicio, L. Sugiyama, R. Granetz, D. A. Gates, J. E. Rice, M. L. Reinke, M. Bitter, E. Fredrickson, C. Gao, M. Greenwald, K. Hill, A. Hubbard, J. W. Hughes, E. Marmar, N. Pablant, Y. Podpaly, S. Scott, R. Wilson, S. Wolfe, and S. Wukitch, Phys. Rev. Letters, **110**, 065006, (2013).

[5] L. Delgado-Aparicio, L Sugiyama, R. Granetz, D. Gates, J. Rice, M. L. Reinke, W. Bergerson, M. Bitter1, D. L. Brower, E. Fredrickson, C. Gao, M. Greenwald, K. Hill, A. Hubbard, J. Irby, J. W. Hughes, E. Marmar, N. Pablant, S. Scott, R. Wilson, S. Wolfe and S. Wukitch, Nucl. Fusion, **53**, 043019, (2013).

[6] D. Pfefferle J. P. Graves, W. A. Cooper, C. Misev, I. T. Chapman, M. Turnyanskiy and S. Sangaroon Nucl. Fusion, **54**, 064020, (2014).

[7] L. Delgado-Aparicio, S. Shiraiwa, L. Sugiyama, R. Parker, S. G. Baek, R. Mumgaard, R. Granetz, I. Faust, S. Scott, D. A. Gates, N. Gorelenkov, N. Bertelli, M. Bitter, C. Gao, M. Greenwald, K. Hill, A. Hubbard, J. Hughes, J. Irby, E. Marmar, O. Meneghini, N. Pablant, P. Phillips, J. E. Rice, W. Rowan, J. Walk, G. Wallace, R. Wilson, S. Wolfe, and S. Wukitch, Proceedings of the 40^{th} European Physical Society, P1.159, Helsinki, Finland, (2013).

[8] L. Delgado-Aparicio, S. Shiraiwa, L. Sugiyama, R. Parker, R. Granetz, S. G. Baek, R. Mumgaard, I. Faust, S. Scott, N. Gorelenkov, N. Bertelli, C. Gao, M. Greenwald, A. Hubbard, J. Hughes, J. Irby, E. Marmar, P. Phillips, J. E. Rice, G. Wallace, R. Wilson, S. Wolfe and S. Wukitch, Proceedings of the 55^{th} Annual Meeting of the APS Division of Plasma Physics, (2013).

[9] L. Sugiyama and L. Delgado-Aparicio, in preparation, to be submitted to Phys. Plasmas, (2015).

[10] Alcator C-Mod Team, Fusion Sci. Technol., **51**, 3, (2007).

[11] P. T. Bonoli, J. Ko, R. Parker, A. E. Schmidt, G. Wallace, J. C. Wright, C. L. Fiore, A. E. Hubbard, J. Irby, E. Marmar, M. Porkolab, D. Terry, S. M. Wolfe, S. J. Wukitch, the Alcator C-Mod Team, J. R. Wilson, S. Scott, E. Valeo, C. K. Phillips, and R. W. Harvey, *et al.*, Phys. Plasmas, **15**, 056117, (2008).

[12] J. R. Wilson, R. Parker, M. Bitter, P. T. Bonoli, C. Fiore, R. W. Harvey, K. Hill, A. E. Hubbard, J. W. Hughes, A. Ince-Cushman, C. Kessel, J. S. Ko, O. Meneghini, C. K. Phillips, M. Porkolab, J. Rice, A. E. Schmidt, S. Scott, S. Shiraiwa, E. Valeo, G. Wallace, J. C. Wright and the Alcator C-Mod Team, *et al.*, Nucl. Fusion, **49**, 115015, (2009).

[13] G. M. Wallace, A. E. Hubbard, P. T. Bonoli, I. C. Faust, R. W. Harvey, J. W. Hughes, B. L. LaBombard, O. Meneghini, R. R. Parker, A. E. Schmidt, S. Shiraiwa, A. P. Smirnov, D. G. Whyte, J. R. Wilson, J. C. Wright, S. J. Wukitch and the Alcator C-Mod Team, *et al.*, Nucl. Fusion, **51**, 083032, (2011).

[14] M. L. Reinke, Y. A. Podpaly, M. Bitter, I. H. Hutchinson, J. E. Rice, L. Delgado-Aparicio, C. Gao, M. Greenwald, K. Hill, N. T. Howard, A. Hubbard, J. W. Hughes, N. Pablant, A. E. White, and S. M. Wolfe, Rev. Sci. Instrum., **83**, 113504, (2012)

[15] L. Delgado-Aparicio, M. Bitter, Y. Podpaly, J. E. Rice, W. Burke, M. Sanchez del Rio, P. Beiersdorfer, R. Bell, R. Feder, C. Gao, K. Hill, D. Johnson, S. G. Lee, E. Marmar, N. Pablant, M. L. Reinke, S. Scott and R. Wilson, Plasma Phys. Control. Fusion, **55**, 125011, (2013).

[16] R. White, The Theory of Toroidally Confined Plasmas, Imperial College Press, (2006).

[17] C. P. Kasten, J. H. Irby, R. Murray, A. E. White and D. C. Pace, *et al.*, Rev. Sci. Instrum., **83**, 10E301, (2012).

[18] J. W. Heard, C. Watts, R. F. Gandy, P. E. Phillips, G. Cima, R. Chatterjee, A. Blair, A. Hubbard, C. W. Domier and N. C. Luhmann Jr., Rev. Sci. Instrum., **70**, 1010, (1999).

[19] R. Chatterjee, P. E. Phillips, J. Heard, C. Watts, R. Gandy and A. Hubbard, Fusion Engineering and Design, **53**, 113, (2001).

[20] T. C. Luce, P. C. Efthimion and N. J. Fisch, Rev. Sci. Instrum., **59**, 1593, (1988).

[21] R. W. Harvey, M. R. O'Brien, V. V. Rozhdestvensky, T. C. Luce, M. G. McCoy and G. D. Kerbel, Phys. Fluids B, **5**, 446, (1993).

[22] S. Preische, P. C. Efthimion and S. M. Kaye, Phys. Plasmas, **3**, 4065, (1996).

[23] S. Coda, Rev. Sci. Intrum., **79**, 10F501, (2008).

[24] K. Hizanidis and A. Bers, Phys. Fluids, **27**, 2669, (1984).

[25] R. W. Harvey and M. McCoy, Proc. IAEA Technical Committee Meeting on Simulation and Modeling of Thermonuclear Plasmas (Montreal, Canada) pp 489, (1992).

[26] K. L. Wong, M. S. Chu, T. C. Luce, C. C. Petty, P. A. Politzer, R. Prater, L. Chen, R. W. Harvey, M. E. Austin, L. C. Johnson, R. J. La Haye, and R. T. Snider, Phys. Rev. Letters, **85**, 996 (2000).

[27] R. Cesario, L. Panaccione, A. Botrugno, G. Calabro, A. Cardinali, C. Castaldo, M. Marinucci, V. Pericoli, A. Romano, P. Smeulders, A. A. Tuccillo and F. Zonca, Nucl. Fusion, **49**, 075034, (2009).

[28] P. Maget, F. Imbeaux, G. Giruzzi, V. S. Udintsev, G. T. A. Huysmans, J.-L. Segui, M. Goniche, Ph. Moreau, R. Sabot and X. Garbet, Nucl. Fusion, **46**, 797, (2006).

[29] A. Macor, M. Goniche, J. F. Artaud, J. Decker, D. Elbeze, X. Garbet, G. Giruzzi, G. T. Hoang, P. Maget, D. Mazon, D. Molina, C. Nguyen, Y. Peysson, R. Sabot, and J. L. Segui, Phys. Rev. Letters, **102**, 155005, (2009).

[30] Z. O. Guimaraes-Filho, D. Elbeze, R. Sabot, D. Molina, J-L Segui, C. Nguyen, J. Decker, P. Maget, A. Merle, X. Garbet, N. Dubuit and S. Benkadda, Plasma Phys. Control. Fusion, **53**, 074012, (2011); Z. O. Guimaraes-Filho, S. Benkadda, D. Elbeze, A. Botrugno, P. Buratti, G. Calabro, J. Decker, N. Dubuit, X. Garbet, P. Maget, A. Merle, G. Pucella, R. Sabot, A. A. Tuccillo and F. Zonca, Nucl. Fusion, **52**, 094009, (2012).

[31] Y. Sun, B. Wan, L. Hu, S. Wang, B. Shen, X. Zhang, X. Zhen and G. Xu, Plasma Phys. Control. Fusion, **47**, 745, (2005).

[32] L. Xu, L. Hu, E. Li, K. Chen and Z. Liu, Phys. Scr., **86**, 039502, (2012).

[33] L.-W. Yan, J.-Q. Dong, X.-T. Ding, Y. Liu, G.-C. Guo, E.-Y. Wang and the HL-1M team, Chinese Phys. Lett., **18**, 1227,

(2001).
[34]W. Chen, X. T. Ding, Yi. Liu, G. L. Yuan, Y. P. Zhang, Y. B. Dong , X. Y. Song, J. Zhou, X. M. Song, W. Deng, Q. W. Yang, X. Q. Ji, X. R. Duan, Y. Liu and the HL-2A Team, Nucl. Fusion, **49**, 075022, (2009); W. Chen, X. T. Ding, Yi. Liu, Q. W. Yang, X. Q. Ji, M. Isobe, G. L. Yuan, Y. P. Zhang, Y. Zhou, X. Y. Song, Y. B. Dong, W. Li, J. Zhou, G. J. Lei, J. Y. Cao, W. Deng, X. M. Song, X. R. Duan and HL-2A Team, Nucl. Fusion, **50**, 084008, (2010).
[35]Li-Qing Xu, Li-Qun Hu and EAST team, Chinese Phys. Lett., **30**, 075201, (2013).
[36]J. Kamleitner, S. Coda, J. Decker, J. P. Graves, S. Gnesin, Proceedings of the 40^{th} European Physical Society, P5.127, Helsinki, Finland, (2013).
[37]Y. Sun, B. Wan, S. Wang, D. Zhou, L. Hu, and B. Shen, Phys. Plasmas, **12**, 092507, (2005).
[38]Z.-T. Wang, Y.-X. Long, J.-Q. Dong, L. Wang, F. Zonca, Chinese Phys. Lett., **23**, 158, (2006).
[39]F. Zonca, P. Buratti, A. Cardinali, L. Chen, J.-Q. Dong, Y.-X. Long, A. V. Milovanov, F. Romanelli, P. Smeulders, L. Wang, Z.-T. Wang, C. Castaldo, R. Cesario, E. Giovannozzi, M. Marinucci and V. Pericoli Ridolfini, Nucl. Fusion, **47** , 1588, (2007).
[40]A. Merle, J. Decker, X. Garbet, R. Sabot, Z. Guimaraes-Filho, and T. Nicolas, Phys. Plasmas, **19**, 072504, (2012).
[41]Shao-Yong Chen, Zhong-Tian Wang and Chang-Jian Tang, Chinese Phys. Lett., **29**, 025203, (2012).
[42]G. Vlad, S. Briguglio, G. Fogaccia, F. Zonca, V. Fusco and X. Wang, Nucl. Fusion, **53**, 083008, (2013).
[43]R. Betti and J. P. Freidberg, Phys. Rev. Letters, **70**, 3428, (1993).